

MUSE: Multi-Subject Unified Synthesis via Explicit Layout Semantic Expansion

Fei Peng^{1,2*} Junqiang Wu^{2*} Yan Li^{2†} Tingting Gao² Di Zhang² Huiyuan Fu^{1†}

¹Beijing University of Posts and Telecommunications, China ²Kuaishou Technology

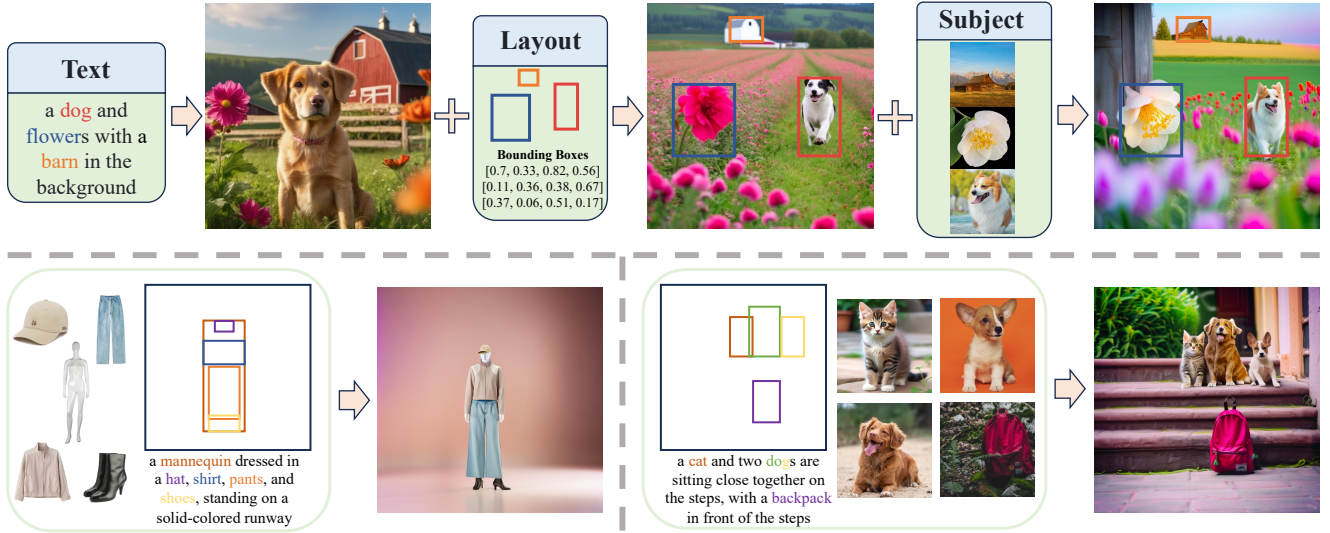


Figure 1. Our MUSE method progressively enhances the control capability of text-to-image model, from layout to subject synthesis. It is versatile to tasks such as precise customization of different parts of a single subject or synthesizing multiple subjects in one image.

Abstract

Existing text-to-image diffusion models have demonstrated remarkable capabilities in generating high-quality images guided by textual prompts. However, achieving multi-subject compositional synthesis with precise spatial control remains a significant challenge. In this work, we address the task of layout-controllable multi-subject synthesis (LMS), which requires both faithful reconstruction of reference subjects and their accurate placement in specified regions within a unified image. While recent advancements have separately improved layout control and subject synthesis, existing approaches struggle to simultaneously satisfy the dual requirements of spatial precision and identity preservation in this composite task. To bridge this gap, we propose MUSE, a unified synthesis framework that employs concatenated cross-attention (CCA) to seamlessly integrate layout specifications with textual guidance through explicit semantic space expansion. The proposed CCA mechanism enables bidirectional modality alignment between spatial constraints and textual descriptions without interference. Furthermore, we design a progressive two-stage training

strategy that decomposes the LMS task into learnable sub-objectives for effective optimization. Extensive experiments demonstrate that MUSE achieves zero-shot end-to-end generation with superior spatial accuracy and identity consistency compared to existing solutions, advancing the frontier of controllable image synthesis. Our code and model are available at <https://github.com/pf0607/MUSE>.

1. Introduction

Recent advances in text-to-image generation [4, 6, 8, 11, 12, 17, 36, 39, 40, 43, 45] built upon diffusion models [11, 22, 48, 49] have demonstrated unprecedented capabilities in synthesizing photorealistic images from textual descriptions. The emergence of architectural innovations like Stable Diffusion [43] has particularly enabled efficient high-resolution generation while maintaining strong text-image alignment. However, achieving precise spatial control over multiple visual elements remains an open challenge, as current models often struggle to faithfully reconstruct specific subjects and position them in designated image regions through textual prompts alone.

This limitation motivates our investigation of layout-controllable multi-subject synthesis (LMS) - a critical task

*Equal contribution. †Corresponding author.

requiring simultaneous satisfaction of two objectives: 1) accurate reconstruction of multiple subjects with identity preservation, and 2) strict adherence to user-specified spatial arrangements within a unified image. The LMS task holds significant practical value for applications ranging from graphic design to interactive storytelling, where precise control over both visual content and composition is essential. Current approaches addressing these requirements can be categorized into two distinct research directions, each with inherent limitations when applied to LMS.

Existing layout control methods primarily adopt two paradigms. Training-free techniques [3, 7, 9, 13, 24, 58, 59] achieve spatial control through post-hoc fusion of independently generated instances during inference, but suffer from inconsistent lighting and perspective across regions. Condition-driven approaches [1, 10, 14, 23, 29, 53, 56, 61, 65] incorporate spatial constraints via additional control modules during training, yet typically lack explicit mechanisms for reference-based subject synthesis. Conversely, subject-driven generation methods [15, 26, 32, 35, 37, 44, 50, 52, 60, 63] excel at reconstructing individual or multiple subjects through textual inversion or adapter networks, but fail to scale effectively to multi-subject scenarios with precise layout requirements. Recent hybrid attempts [29, 54] to combine these capabilities reveal fundamental architectural limitations: parameter-intensive fusion mechanisms [29] become computationally prohibitive at scale, while decoupled cross-attention approaches [54] exhibit control collision between layout and text conditions.

To overcome these limitations, we present MUSE (Multi-Subject Unified Synthesis via Explicit Layout Semantic Expansion), a novel framework that achieves precise layout control and identity-preserving subject synthesis through three key innovations. First, we introduce concatenated cross-attention (CCA), an explicit semantic space expansion mechanism that enables bidirectional alignment between layout specifications and textual guidance without interference. Second, we develop a progressive two-stage training strategy that decouples layout control learning from subject synthesis optimization, effectively mitigating control collision during joint training. Third, our architecture requires no test-time fine-tuning while supporting zero-shot generation of complex multi-subject compositions.

Our primary contributions are threefold: 1) We identify key technical barriers preventing existing methods from achieving layout-controllable multi-subject synthesis (LMS) and propose an efficient LMS framework—MUSE. 2) We propose an explicit layout semantic expansion method that leverages the newly introduced concatenated cross-attention to enable compatibility between layout control and text control, achieving more precise and effective layout-controllable image generation. 3) We devise a progressive training paradigm that decomposes the LMS ob-

jective into sequential layout control acquisition and subject synthesis refinement phases, effectively resolving optimization conflicts inherent in joint training.

Extensive quantitative evaluations and ablation studies demonstrate that MUSE achieves state-of-the-art performance in both layout accuracy and subject fidelity, while maintaining efficient generation speeds. Our framework establishes new capabilities for controllable image synthesis, significantly advancing the practical deployment of diffusion models in professional design workflows.

2. Related Work

Text-to-Image Generation [2, 4–6, 8, 11, 12, 16, 17, 22, 33, 36, 39–41, 43, 45, 48, 49] utilize text as control conditions to generate images that meet specified requirements. In recent years, diffusion models [11, 22, 48, 49] have demonstrated impressive performance in image generation, but their efficiency is compromised due to the necessity of multiple steps of noise prediction in pixel space. Latent Diffusion Model (LDM) [43] improves this issue by integrating Variational Auto-Encoder (VAE) [25] technique to conduct the denoising process in a compressed latent space, significantly enhancing the efficiency of image diffusion models.

Layout Control for Image Generation serves as a complement to the text control by providing additional layout conditions, such as segmentation masks and bounding boxes. Training-free methods [3, 7, 9, 13, 24, 58, 59] introduce layout guidance operations during inference on pre-trained generation models. For example, MultiDiffusion [3], NoiseCollage [47] and SceneDiffusion [42] denoise each instance separately and then perform a fusion of the multiple instances. Additionally, some methods [1, 10, 14, 23, 29, 53, 56, 61, 65] fine-tune pre-trained models to accept layout control conditions. Make-a-scene [14], Spa-text [1], ControlNet [61] and Anydoor [10] utilize segmentation masks to generate images that conform to the shapes defined by these masks. GLIGEN [29], InstanceDiffusion [53], MIGC [64, 65] and IFAdapter [56] allow for more flexible layout control by accepting various layout conditions, such as bounding boxes, points, and masks.

Subject Synthesis has made significant progress in single-subject methods [15, 19, 26, 28, 37, 44, 52, 55, 60]. Dreambooth [44] binds reference images to specific labels and fine-tunes the U-Net. IP-Adapter [60] utilizes CLIP [38] to encode reference images and trains additional decoupled attention networks to inject image control. InstantID [52] enhances facial personalization by incorporating an additional face encoder. Real-Custom [23] constructs an adaptive module to select appropriate encoded image features. Multi-subject synthesis has attracted increasing research interest. Custom Diffusion [27] reduces the parameter update requirements of DreamBooth, allowing multiple subjects to be bound to different labels simultaneously. Mix-of-Show

[18] binds multiple subjects by additionally training LoRA. Zero-shot methods [32, 34, 35, 50, 54, 57, 63] are simpler and more practical for real-world applications. SSRencoder [63] extracts subject features from images by relating them to the corresponding text in the prompt. λ -eclipse [35] maps encoded reference image and text features into the same representation in the latent space. MultiGen [57] fine-tunes the pre-trained generative model to incorporate multi-modal control. MS-Diffusion [54] and SubjectDiffusion [32] fuse the subject images and coordinates through a network and then inject them via adapters.

3. Method

3.1. Preliminaries

Stable Diffusion [43] is a commonly used text-to-image diffusion model that performs diffusion operations in a compressed latent space to improve the efficiency of high-resolution image generation. In UNet, cross-attention (CA) layers are designed specifically to receive control conditions. Formally, let Q denote the query obtained by projecting the unfolded latent space image features via a linear layer, and K, V represent the key and value derived by projecting the features encoded from the control text by CLIP [38]. The token dimension of K is d . σ denotes the softmax operation. The CA is calculated as follows:

$$CA = \sigma \left(\frac{QK^T}{\sqrt{d}} \right) V. \quad (1)$$

Decoupled cross-attention (DCA) is a commonly used method for plugin-based injection of additional control conditions. It operates by freezing the pre-trained UNet and training additional linear layers within the original CA layer to project encoded additional control features into key and value. Then compute new CA with the pre-trained query and add the result to original text-driven CA result. For instance, in a subject synthesis task, the calculation of DCA can be formulated as:

$$DCA = \sigma \left(\frac{QK^T}{\sqrt{d}} \right) V + \lambda \cdot \sigma \left(\frac{QK_I^T}{\sqrt{d}} \right) V_I. \quad (2)$$

K_I and V_I are the key and value projected from the image features. λ is the adjustable control strength scale, typically taking values between 0 and 1. DCA effectively leverages the prior knowledge of the pre-trained model, allowing for efficient training with minimal increase in parameter count.

3.2. Overview

Task Definition. In this paper, we introduce the layout-controllable multi-subject synthesis (LMS) task. We define the input control conditions as follows: the global prompt text, along with additional inputs for N subjects, which include each subject’s reference image, bounding box coordinates, and class text. These inputs are denoted as $T_{\text{global}}, I_i,$

$B_i,$ and T_i for $1 \leq i \leq N$, respectively. The image generation model is required to produce an image that not only aligns with T_{global} but also ensures that each subject appears in its specified B_i and resembles the corresponding I_i .

Limitations. Current methods that incorporate these conditions simultaneously have notable limitations. GLIGEN [29] adds new gated self-attention (SA) layers between the SA and CA layers of the UNet to accept control inputs, which significantly increases the size of the diffusion model (e.g., SDXL grows from 2.56B to 4.3B), making it overly burdensome and difficult to train as current model sizes continue to increase. Existing commonly used control methods [52, 54, 56, 60, 63–65] typically use lighter-weight DCA method that is compatible with pre-trained models and has been successfully applied in larger models like SDXL [36]. MS-Diffusion [54] uses DCA on the SDXL model to explore LMS tasks and demonstrates some effectiveness. However, we observe that its layout control capability is relatively poor. This limitation arises partly due to the control collision issue associated with the DCA method, as discussed in Sec. 3.3, and partly because layout control and multi-subject synthesis are two challenging sub-tasks to reconcile effectively during training.

Proposed method. To enable effective LMS, we propose the MUSE framework. We decompose the task into two progressive stages. First, we propose an explicit layout semantic expansion method that enables compatibility between layout and text controls, achieving text-aligned, layout-controllable image generation. Second, we further train the subject synthesis DCA network based on the pre-trained layout-controllable generation model. With the combination of the advantages from the two progressive stages, we ultimately obtain an effective zero-shot, end-to-end LMS model.

3.3. Explicit Layout Semantic Expansion for Text

For the standalone layout control task, subject synthesis is not required. Instead, only the additional subject text T_i and subject position B_i are considered. We follow existing methods [29, 53, 54, 56, 65], which typically fuse the encoded features of T_i with the encoded B_i to obtain the final layout control representation, known as the grounding token and denoted as G_T^i . This is calculated as follows:

$$G_T^i = \text{MLP}([f_T^i, \text{Fourier}(B_i)]), \quad (1 \leq i \leq N) \quad (3)$$

where B_i is Fourier encoded and f_T^i is the encoded feature of T_i , often the class token extracted by CLIP [38]. $[\cdot]$ denotes the concatenation operation. Then the concatenated features are fused through a Multi-Layer Perceptron network (MLP). To achieve multi-subject layout control, it is sufficient to concatenate the grounding tokens of all subjects, represented as $G_T = [G_T^1, G_T^2, \dots, G_T^N]$.

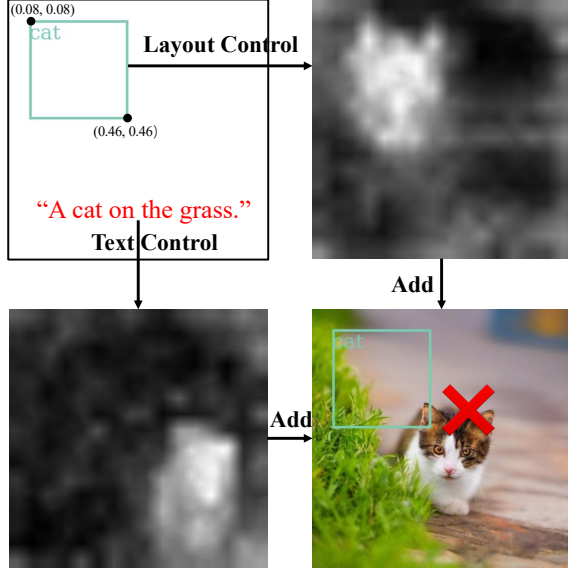


Figure 2. The control collision issue. This occurs when the attention generated by layout control conflicts with that of text control over specific layout regions, ultimately leading to generated images that fail to meet layout control conditions.

Control Collision. Compared to some methods [29, 53] that incorporate large gated SA layers to receive the G_T , other methods [54, 56, 65] using DCA offer higher training and inference efficiency, achieving significant progress in layout control. However, layout control with DCA presents an issue we term control collision: without injected layout control, image generation under a text prompt generally results in random layouts that may be aligned with the broader distribution of training data. When injected layout control information diverges from this data distribution, as shown in Fig. 2, two distinct layouts may emerge from the CA heatmaps of text and layout control, causing collision when combined through element-wise addition in Eq. (2). This results in poor layout control in generated images. Methods like MIGC [65], NoiseCollage [47], and SceneDiffusion [42] try to solve this by separately generating global backgrounds and individual instances before merging, but at a high computational cost, potentially leading to inconsistencies among instances.

Explicit Layout Semantic Expansion. To address control collision, we provide a simpler solution from a semantic perspective: For text-to-image tasks, the global semantics of the generated image should align with the global semantics of the corresponding text. Subject synthesis information is also a form of global image semantics, and DCA effectively applies subject synthesis control information across the entire image through the element-wise addition in Eq. (2) [52, 60], allowing it to align with the text control. However, layout is a type of implicit, local semantic information. Specifically, for the same text, the layout

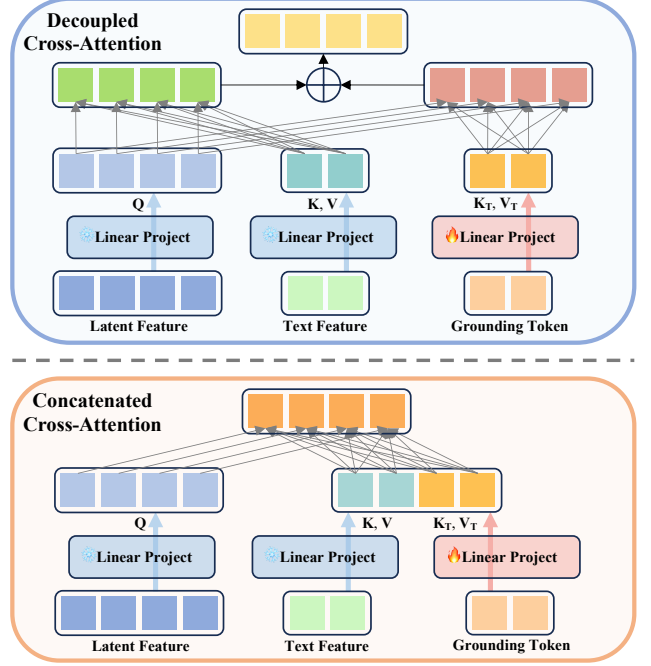


Figure 3. Comparison between decoupled cross-attention (DCA) and concatenated cross-attention (CCA) structures. DCA separately calculates two control attention maps and combines them using element-wise addition. In contrast, CCA integrates the two control conditions through concatenation, computing a single attention map that unifies layout and text control in one step.

across multiple generated images is typically random, yet this randomness doesn’t affect image semantic alignment with the text. Consequently, when using DCA to apply explicit layout control information across the entire image, it may collide with the image’s implicit local layout semantics. A simple method to avoid this collision is to explicitly expand the implicit layout semantic information into the text, which represents the global semantics of the image.

We propose a semantic expansion method via concatenated cross-attention (CCA). As illustrated in Fig. 3, compared to DCA, CCA also adds linear layers within the original CA layer to project G_T to key and value, denoted as K_T and V_T . These are then concatenated with the key and value projections of the encoded text control, and the combined result is computed as follows:

$$\text{CCA} = \sigma \left(\frac{Q[K, K_T]^T}{\sqrt{d}} \right) [V, V_T]. \quad (4)$$

Unlike DCA’s dual computation, CCA considers both text and layout control in a single computation. The purpose of CCA is to expand the text semantics to include explicit layout information. For example, let’s define a text prompt for generating an image as follows:

“A dog and a cat on the grass.”

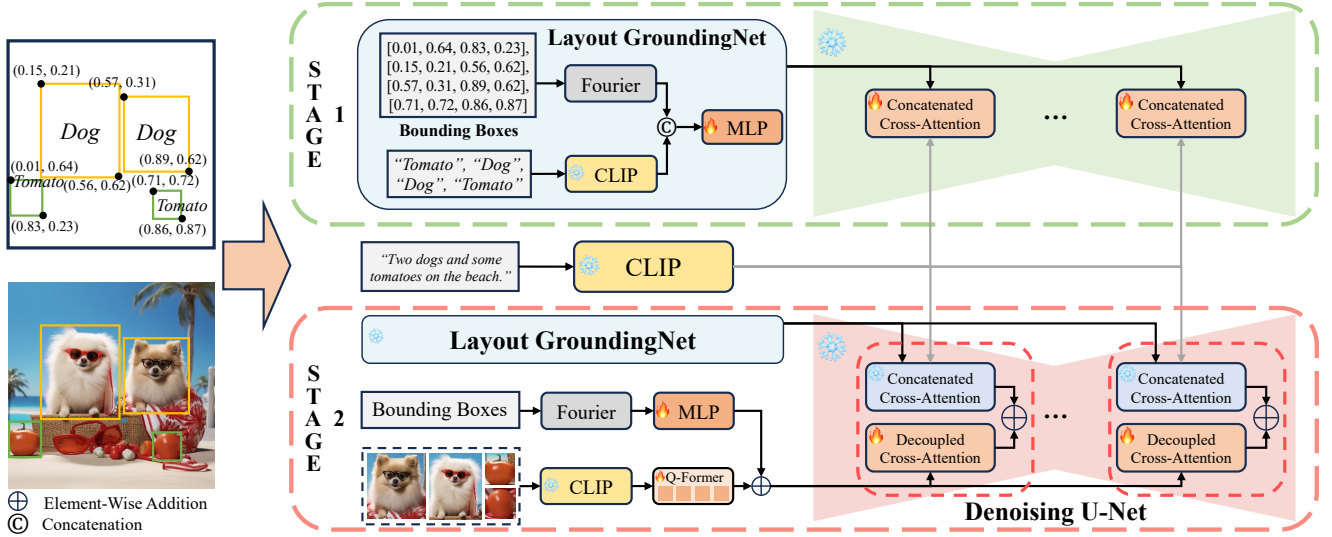


Figure 4. The proposed Progressive Two-Stage Training pipeline. In the first stage, we train the concatenated cross-attention network to incorporate layout control conditions, establishing an accurate layout-controllable generation model. In the second stage, we build on this pre-trained layout model by adding training for subject synthesis. This two-stage strategy results in an effective model for layout-controllable multi-subject synthesis.

We want this text to be explicitly expanded to:

*“A dog and a cat on the grass,
with the cat located at B_{cat} and the dog at B_{dog} .”*

where B_{cat} and B_{dog} represent bounding box coordinates for the cat and dog.

3.4. Decompose LMS into Progressive Stages.

For the complete LMS setup, the grounding token G_I is obtained by replacing the subject text feature f_T^i in Eq. (3) with the encoded subject image feature f_I^i . Different methods [29, 54, 64] vary in the details of generating G_I , and generally, both G_T and G_I are used to enhance performance. Given DCA’s effectiveness in handling subject synthesis, it remains a favorable choice for LMS. MS-Diffusion [54] achieves LMS via DCA. It performs well in subject synthesis but struggles with layout control due to the control collision issue discussed in Sec. 3.3. A straightforward solution involves constructing a composite network that injects G_T via CCA to achieve semantically controlled image layout, while also using DCA to inject G_I for subject synthesis in specified positions. The final calculation of CA in Eq. (1) is modified as follows:

$$\text{FCA} = \sigma \left(\frac{Q[K, K_T]^T}{\sqrt{d}} \right) [V, V_T] + \lambda \cdot \sigma \left(\frac{Q[K_I^T]}{\sqrt{d}} \right) V_I. \quad (5)$$

Progressive Two-Stage Training. In practice, another challenge arises: training for layout control and subject synthesis simultaneously proves difficult, as they are complex and often conflicting sub-tasks. With the integration of CCA, the model’s layout controllability improves, but

subject synthesis tends to suffer. To address this, we decompose the LMS task into a progressive two-stage task. Given the strong compatibility between CCA’s semantic expansion and text control, Stage 1 involves training a CCA-based layout control model. Once the model reaches satisfactory layout controllability, it is frozen, and in Stage 2, DCA is introduced to train the final LMS model. With layout controllability already integrated, Stage 2 training focuses on enhancing subject synthesis. The progressive two-stage training pipeline is depicted in Fig. 4.

End-to-End Inference. With the progressive training strategy, the functionalities of both stages are successfully integrated into a single model, allowing for end-to-end, single-stage inference by simply inputting both G_T and G_I .

Grounding Token Synthesis Improvements. To further enhance detail preservation in subject synthesis, we follow the IP-Adapter-Plus [60] by using a resampler with learnable query tokens. This resampler extracts 4 tokens representing subject image features from the 256 image feature tokens encoded by CLIP. However, using Eq. (3) to fuse multiple tokens of the same subject image individually with the same bounding box disrupts the consistency of image information. We modify the method for obtaining G_T by projecting the encoded bounding box directly to match the image feature token dimensions using a separate MLP, and then directly adding it. The expression is as follows:

$$G_I^i = [\text{MLP}(\text{Fourier}(B_i)) + f_I^{ij}], \quad (1 \leq j \leq 4) \quad (6)$$

where f_I^{ij} represents the encoded features of the same subject image. After being fused with B_i , they are concatenated to form the grounding token G_I for a single subject image.

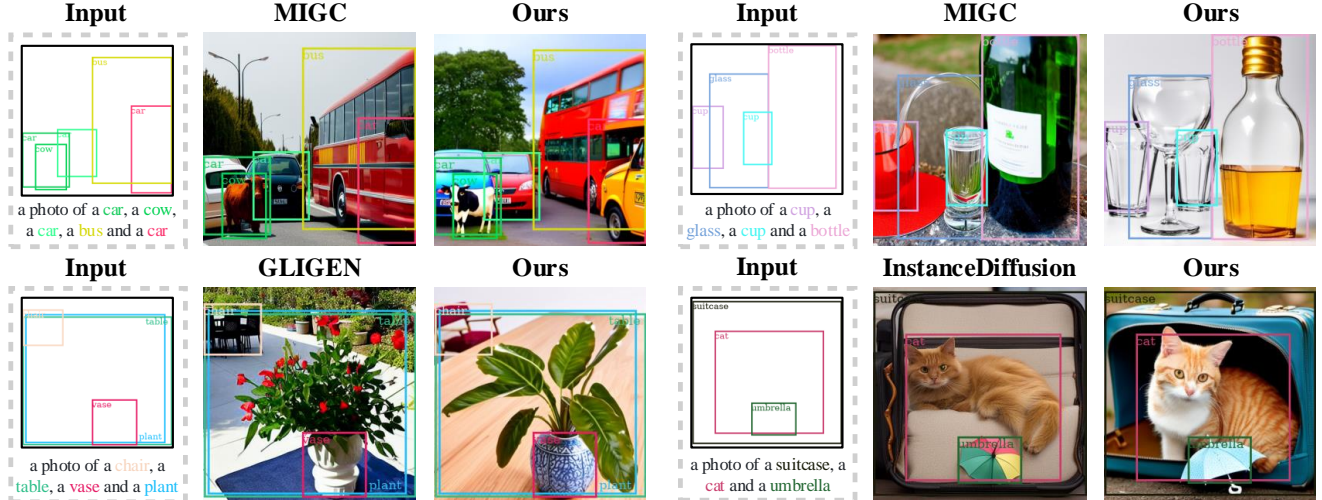


Figure 5. Qualitative experiments on MIG Bench.

4. Experiments

4.1. Implementation Details

Training Data Preparation. We construct training data by randomly sampling 4M image-text pairs from the LAION-5B dataset [46]. To enable precise subject localization, we employ a two-stage annotation process: 1) Subject labeling using the Recognize Anything Model [62], followed by 2) Bounding box generation via Grounding DINO [31]. This pipeline produces cropped subject images with text labels and accurate spatial coordinates.

Experimental Setup. Our MUSE model is built on the pre-trained SDXL [36], utilizing CLIP [38] as both the image and text encoder. For all training stages, we use the AdamW optimizer with a learning rate of 1×10^{-4} . Training is conducted on 64 V100 GPUs, with a batch size of 384, for a total of 100K training steps. Two-stage resolutions of 512 and 1024 are used for training. During inference, we employ the DDIM [48] sampler with 30 steps and set the CFG [21] to 7.5, and for a fair comparison, 512 resolution is used. The DCA control scale λ is empirically set to 0.8.

4.2. Benchmark Datasets and Evaluation Metrics

MIG Bench. The MIG Bench dataset [65], constructed from 800 COCO [30] images, provides holistic text descriptions, instance-level color/class annotations, and bounding boxes for 2–6 instances per image. Its evaluation focuses solely on **layout success rate** (IoU>0.5 for all instances) through Grounding DINO [31]-based detection. This design stems from two considerations: 1) In LMS tasks, instance colors are predefined by reference images rather than text descriptions, making color accuracy assessment irrelevant; 2) Layout fidelity constitutes the core challenge in multi-instance generation. Success rates are categorized by instance count (L2–L6) to analyze model scalability.

Methods	Layout Success Rate (%)						Time (s)
	L2	L3	L4	L5	L6	Avg	
GLIGEN	0.913	0.908	0.877	0.834	0.848	0.866	15.9
InstanceDiffusion	0.931	0.902	0.894	0.839	0.864	0.876	26.5
MIGC	0.934	0.925	0.873	0.850	0.832	0.869	9.1
Ours	0.906	0.917	0.891	0.858	0.878	0.884	4.1

Table 1. Comparative evaluation of layout control performance on MIG Bench. Metrics include layout success rates (IoU>0.5) across instance count levels (L2–L6) and average inference time.

MS-Bench. The MS-Bench dataset [54] contains 1,148 subject combinations (2–3 subjects per image) from 40 distinct classes, paired with bounding boxes and up to 6 text prompts per combination (4,488 total samples). To overcome the limitations of MS-Bench’s rigid layout structure (primarily centered or left-right arrangements with uniform sizing), we propose **MS-Bench-Random**, which introduces randomized subject positions and sizes to better align with the practical requirements of LMS tasks. For evaluation, we measure: 1) **CLIP-T** score [20] for text-image alignment; 2) **CLIP-I-local** score comparing cropped generated regions (using GT bounding boxes) with reference subjects via CLIP-I [38]; 3) **LMS success rate** requiring all subjects to meet CLIP-I-local thresholds (0.6/0.65). This multi-metric approach ensures a comprehensive assessment of spatial accuracy and subject fidelity.

4.3. Quantitative Experiments

Layout Control on MIG Bench. As shown in Tab. 1, all compared methods achieve competent layout success rates (>86.6% on average), demonstrating their effectiveness in addressing control collision issues through other innovations (e.g., GLIGEN’s gated self-attention [29] or MIGC’s divide-and-conquer approach [65]). Our method establishes state-of-the-art performance with an 88.4% average success rate. The advantage becomes particularly pronounced in high-complexity scenarios involving 5–6 in-

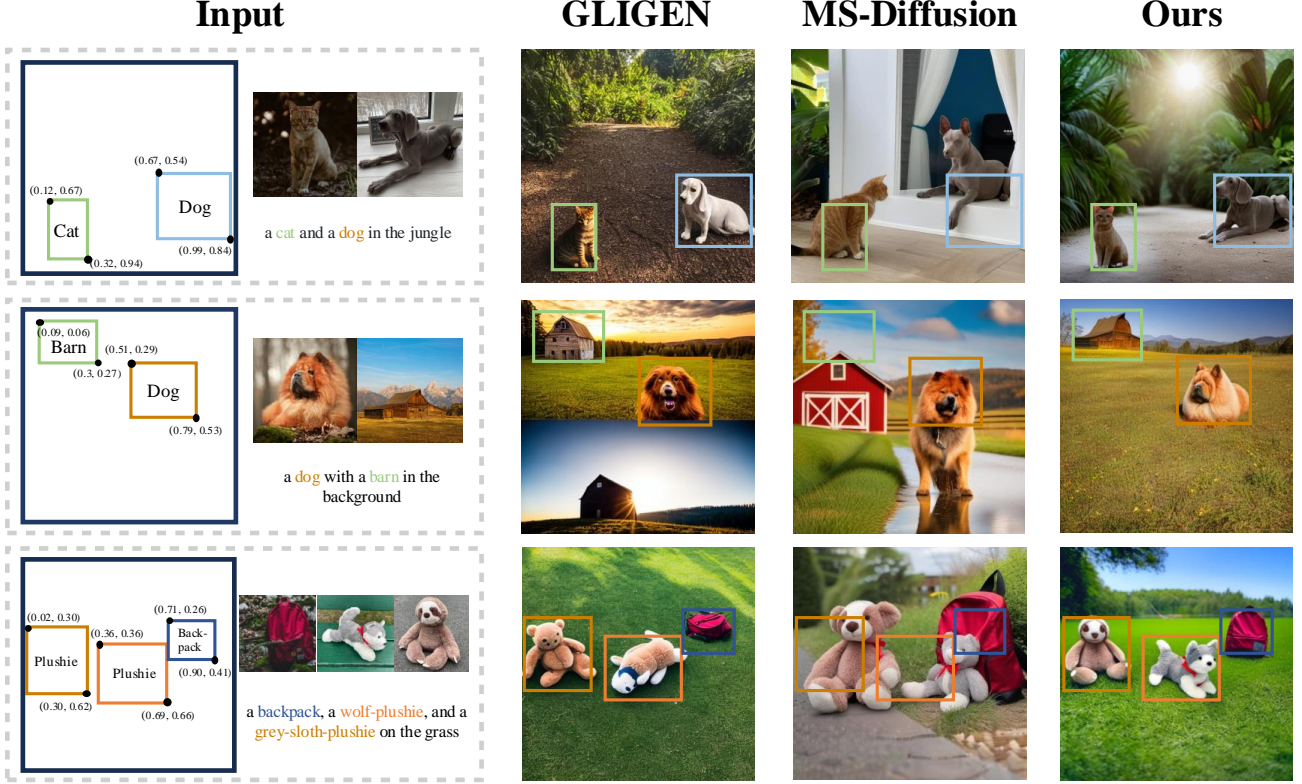


Figure 6. Qualitative experiments on MS-Bench-Random.

Methods	MS-Bench				MS-Bench-Random			
	CLIP-T	CLIP-I-I	SR-0.6	SR-0.65	CLIP-T	CLIP-I-I	SR-0.6	SR-0.65
GLIGEN	0.299	0.799	0.880	0.810	0.297	0.747	0.870	0.682
MS-Diffusion	0.318	0.780	0.820	0.706	0.316	0.686	0.506	0.289
Ours	0.323	0.827	0.890	0.819	0.321	0.779	0.894	0.755

Table 2. LMS performance comparison on MS-Bench. Metrics include text-image alignment (CLIP-T), local subject fidelity (CLIP-I-I), and success rates using CLIP-I-I thresholds of 0.6/0.65 (SR-0.6/SR-0.65), evaluated under fixed and randomized layouts.

stances (L5-L6). This superior scalability stems from our simple yet effective semantic expansion paradigm: The concatenated cross-attention (CCA) mechanism resolves control collisions through unified semantic alignment between layout constraints and textual descriptions, avoiding the need for complex module stacking or massive parameter growth. Notably, our lightweight implementation achieves inference speeds of 4.1s (3.9–6.5× faster than GLIGEN and InstanceDiffusion[53]), while maintaining architectural compatibility for downstream tasks through standardized attention interfaces, as evidenced by the seamless integration of subject synthesis.

LMS Performance on MS-Bench. As Shown in Tab. 2, our method demonstrates remarkable robustness under challenging randomized layouts. While baseline methods like MS-Diffusion [54] suffer catastrophic performance degradation in random conditions (SR-0.65 drops from 70.6% to 28.9%, -41.7%), our approach maintains strong local subject fidelity (CLIP-I-local: 0.779) with only marginal quality reduction (SR-0.65: 75.5%, -6.4% from fixed layout).

This minimal performance decay contrasts sharply with GLIGEN’s 12.8% SR-0.65 decline under equivalent randomization, confirming our MUSE framework effectively combines layout control with subject synthesis. Notably, even with randomized layout, our CLIP-T score (0.321) remains comparable to fixed layouts (0.323), indicating stable text-alignment capability regardless of spatial constraints.

4.4. Qualitative Experiments

Layout Control on MIG Bench. As shown in Fig. 5, we compare our method with existing state-of-the-art methods [29, 53, 65] in terms of layout control. It can be observed that our method is still able to accurately generate images and maintain good quality even in complex layout scenarios. This demonstrates the superiority of the CCA method in balancing layout control and text control.

LMS Performance on MS-Bench-Random. Fig. 6 compares our MUSE model with state-of-the-art LMS methods [29, 54], on the challenging MS-Bench-Random dataset. Our model consistently outperforms baselines in complex



Figure 7. Ablation study on training strategies conducted on MS-Bench-Random.

Methods	CLIP-T	Layout Success Rate					
		L2	L3	L4	L5	L6	Avg
DCA	0.322	0.807	0.801	0.780	0.761	0.756	0.781
CCA	0.331	0.906	0.917	0.891	0.858	0.878	0.884

Table 3. Ablation study comparing attention mechanisms on layout control performance (MIG Bench).

scenarios, achieving precise layout precision while preserving high-fidelity subject details. These results validate MUSE’s effectiveness in real-world applications requiring both spatial accuracy and identity preservation.

4.5. Ablation Experiments

Explicit Layout Semantic Expansion Mechanism. Tab. 3 reveals that replacing decoupled cross-attention (DCA) with our CCA framework improves layout success rates by 10.3% (L2–L6 average) while maintaining superior text alignment (CLIP-T: 0.331 vs 0.322). This confirms CCA’s ability to integrate layout constraints as expanded textual semantics rather than competing control signals.

Progressive Two-Stage Training Strategy. Tab. 4 provides critical insights into the design of training strategies for our MUSE framework. The **full-DCA** approach reveals severe interference when applying DCA for both layout control and subject synthesis, resulting in a 41.0% drop in SR-0.65. The **single-stage CCA+DCA** method reveals the inherent trade-off between concurrent layout and subject optimization: a reduced success rate loss (-33.6% SR-0.65) comes at the expense of degraded subject fidelity (-0.085 CLIP-I-I). **Joint training**, which simultaneously optimizes both layout and subject objectives throughout the second training stage, achieves moderate success (-4.3% SR-0.65). The **Reversed training** strategy, which prioritizes subject synthesis before layout control, proves catastrophic for spatial reasoning, as evidenced by a 0.056 CLIP-I-I gap (-7.2%) compared to our approach. Our progressive two-stage strategy resolves these issues through ordered parameter freezing: CCA-first

Methods	CLIP-T	CLIP-I-I	SR-0.6	SR-0.65
Full-DCA	-0.013	-0.076	-0.309	-0.410
Single Stage	-0.008	-0.085	-0.227	-0.336
Joint Training	-0.005	-0.022	-0.017	-0.043
Reversed Training	-0.008	-0.056	-0.043	-0.084
Concatenated Grounding	-0.003	-0.015	-0.008	-0.021
Ours	0.321	0.779	0.894	0.755

Table 4. Ablation study on training strategies under randomized layouts (MS-Bench-Random).

training establishes robust spatial priors, enabling subsequent DCA-based subject refinement in the second stage without control collision. The subject similarity of the **concatenated grounding** method in Eq. (3) decreases (-0.015 CLIP-I-I while only -0.8% SR-0.6), demonstrating our proposed grounding method in Eq. (6) better maintains internal consistency among multiple image tokens of the subject.

Fig. 7 qualitatively evaluates our progressive two-stage LMS framework against full-DCA and single-stage CCA+DCA methods on MS-Bench-Random. Our approach uniquely achieves precise layout control and high-fidelity subject synthesis, demonstrating superior suitability for LMS tasks compared to competing training strategies.

5. Conclusion

In this research, we introduce MUSE, a novel framework addressing LMS task. Our method decomposes the complex LMS task into a progressive, two-stage sub-task. We first introduce the CCA method, which enhances the model’s compatibility between layout and text control by explicitly expanding the layout semantic for text, effectively resolving control collision. Building upon this enhanced layout control model, we employ the DCA method to enable multi-subject synthesis, achieving zero-shot LMS without modifying pre-trained models. Extensive experiments validate the effectiveness of MUSE, demonstrating its superior performance on LMS tasks and valuable contribution to enhancing control ability in text-to-image diffusion models.

References

- [1] Omri Avrahami, Thomas Hayes, Oran Gafni, Sonal Gupta, Yaniv Taigman, Devi Parikh, Dani Lischinski, Ohad Fried, and Xi Yin. Spatext: Spatio-textual representation for controllable image generation. In *Proceedings of the IEEE/CVF Conference on Computer Vision and Pattern Recognition*, pages 18370–18380, 2023. 2
- [2] Yogesh Balaji, Seungjun Nah, Xun Huang, Arash Vahdat, Jiaming Song, Qingsheng Zhang, Karsten Kreis, Miika Aittala, Timo Aila, Samuli Laine, et al. ediff-i: Text-to-image diffusion models with an ensemble of expert denoisers. *arXiv preprint arXiv:2211.01324*, 2022. 2
- [3] Omer Bar-Tal, Lior Yariv, Yaron Lipman, and Tali Dekel. Multidiffusion: Fusing diffusion paths for controlled image generation. 2023. 2
- [4] James Betker, Gabriel Goh, Li Jing, Tim Brooks, Jianfeng Wang, Linjie Li, Long Ouyang, Juntang Zhuang, Joyce Lee, Yufei Guo, et al. Improving image generation with better captions. *Computer Science*. <https://cdn.openai.com/papers/dall-e-3.pdf>, 2(3):8, 2023. 1, 2
- [5] Andrew Brock. Large scale gan training for high fidelity natural image synthesis. *arXiv preprint arXiv:1809.11096*, 2018.
- [6] Huiwen Chang, Han Zhang, Jarred Barber, AJ Maschinot, Jose Lezama, Lu Jiang, Ming-Hsuan Yang, Kevin Murphy, William T Freeman, Michael Rubinstein, et al. Muse: Text-to-image generation via masked generative transformers. *arXiv preprint arXiv:2301.00704*, 2023. 1, 2
- [7] Hila Chefer, Yuval Alaluf, Yael Vinker, Lior Wolf, and Daniel Cohen-Or. Attend-and-excite: Attention-based semantic guidance for text-to-image diffusion models. *ACM Transactions on Graphics (TOG)*, 42(4):1–10, 2023. 2
- [8] Junsong Chen, Jincheng Yu, Chongjian Ge, Lewei Yao, Enze Xie, Yue Wu, Zhongdao Wang, James Kwok, Ping Luo, Huchuan Lu, et al. Pixart- α : Fast training of diffusion transformer for photorealistic text-to-image synthesis. *arXiv preprint arXiv:2310.00426*, 2023. 1, 2
- [9] Minghao Chen, Iro Laina, and Andrea Vedaldi. Training-free layout control with cross-attention guidance. In *Proceedings of the IEEE/CVF Winter Conference on Applications of Computer Vision*, pages 5343–5353, 2024. 2
- [10] Xi Chen, Lianghua Huang, Yu Liu, Yujun Shen, Deli Zhao, and Hengshuang Zhao. Anydoor: Zero-shot object-level image customization. In *Proceedings of the IEEE/CVF Conference on Computer Vision and Pattern Recognition*, pages 6593–6602, 2024. 2
- [11] Prafulla Dhariwal and Alexander Nichol. Diffusion models beat gans on image synthesis. *Advances in neural information processing systems*, 34:8780–8794, 2021. 1, 2
- [12] Patrick Esser, Sumith Kulal, Andreas Blattmann, Rahim Entezari, Jonas Müller, Harry Saini, Yam Levi, Dominik Lorenz, Axel Sauer, Frederic Boesel, et al. Scaling rectified flow transformers for high-resolution image synthesis. In *Forty-first International Conference on Machine Learning*, 2024. 1, 2
- [13] Weixi Feng, Xuehai He, Tsu-Jui Fu, Varun Jampani, Arjun Akula, Pradyumna Narayana, Sugato Basu, Xin Eric Wang, and William Yang Wang. Training-free structured diffusion guidance for compositional text-to-image synthesis. *arXiv preprint arXiv:2212.05032*, 2022. 2
- [14] Oran Gafni, Adam Polyak, Oron Ashual, Shelly Sheynin, Devi Parikh, and Yaniv Taigman. Make-a-scene: Scene-based text-to-image generation with human priors. In *European Conference on Computer Vision*, pages 89–106. Springer, 2022. 2
- [15] Rinon Gal, Yuval Alaluf, Yuval Atzmon, Or Patashnik, Amit H Bermano, Gal Chechik, and Daniel Cohen-Or. An image is worth one word: Personalizing text-to-image generation using textual inversion. *arXiv preprint arXiv:2208.01618*, 2022. 2
- [16] Ian Goodfellow, Jean Pouget-Abadie, Mehdi Mirza, Bing Xu, David Warde-Farley, Sherjil Ozair, Aaron Courville, and Yoshua Bengio. Generative adversarial networks. *Communications of the ACM*, 63(11):139–144, 2020. 2
- [17] Shuyang Gu, Dong Chen, Jianmin Bao, Fang Wen, Bo Zhang, Dongdong Chen, Lu Yuan, and Baining Guo. Vector quantized diffusion model for text-to-image synthesis. In *Proceedings of the IEEE/CVF conference on computer vision and pattern recognition*, pages 10696–10706, 2022. 1, 2
- [18] Yuchao Gu, Xintao Wang, Jay Zhangjie Wu, Yujun Shi, Yunpeng Chen, Zihan Fan, Wuyou Xiao, Rui Zhao, Shuning Chang, Weijia Wu, et al. Mix-of-show: Decentralized low-rank adaptation for multi-concept customization of diffusion models. *Advances in Neural Information Processing Systems*, 36:15890–15902, 2023. 3
- [19] Ligong Han, Yinxiao Li, Han Zhang, Peyman Milanfar, Dimitris Metaxas, and Feng Yang. Svdif: Compact parameter space for diffusion fine-tuning. In *Proceedings of the IEEE/CVF International Conference on Computer Vision*, pages 7323–7334, 2023. 2
- [20] Jack Hessel, Ari Holtzman, Maxwell Forbes, Ronan Le Bras, and Yejin Choi. Clipscore: A reference-free evaluation metric for image captioning. *arXiv preprint arXiv:2104.08718*, 2021. 6
- [21] Jonathan Ho and Tim Salimans. Classifier-free diffusion guidance. *arXiv preprint arXiv:2207.12598*, 2022. 6
- [22] Jonathan Ho, Ajay Jain, and Pieter Abbeel. Denoising diffusion probabilistic models. *Advances in neural information processing systems*, 33:6840–6851, 2020. 1, 2
- [23] Mengqi Huang, Zhendong Mao, Mingcong Liu, Qian He, and Yongdong Zhang. Realcustom: narrowing real text word for real-time open-domain text-to-image customization. In *Proceedings of the IEEE/CVF Conference on Computer Vision and Pattern Recognition*, pages 7476–7485, 2024. 2, 1
- [24] Yunji Kim, Jiyoung Lee, Jin-Hwa Kim, Jung-Woo Ha, and Jun-Yan Zhu. Dense text-to-image generation with attention modulation. In *Proceedings of the IEEE/CVF International Conference on Computer Vision*, pages 7701–7711, 2023. 2
- [25] Diederik P Kingma. Auto-encoding variational bayes. *arXiv preprint arXiv:1312.6114*, 2013. 2

- [26] Jing Yu Koh, Daniel Fried, and Russ R Salakhutdinov. Generating images with multimodal language models. *Advances in Neural Information Processing Systems*, 36, 2024. 2
- [27] Nupur Kumari, Bingliang Zhang, Richard Zhang, Eli Shechtman, and Jun-Yan Zhu. Multi-concept customization of text-to-image diffusion. In *Proceedings of the IEEE/CVF Conference on Computer Vision and Pattern Recognition*, pages 1931–1941, 2023. 2
- [28] Dongxu Li, Junnan Li, and Steven Hoi. Blip-diffusion: Pre-trained subject representation for controllable text-to-image generation and editing. *Advances in Neural Information Processing Systems*, 36:30146–30166, 2023. 2
- [29] Yuheng Li, Haotian Liu, Qingyang Wu, Fangzhou Mu, Jianwei Yang, Jianfeng Gao, Chunyuan Li, and Yong Jae Lee. Gligen: Open-set grounded text-to-image generation. In *Proceedings of the IEEE/CVF Conference on Computer Vision and Pattern Recognition*, pages 22511–22521, 2023. 2, 3, 4, 5, 6, 7, 1
- [30] Tsung-Yi Lin, Michael Maire, Serge Belongie, James Hays, Pietro Perona, Deva Ramanan, Piotr Dollár, and C Lawrence Zitnick. Microsoft coco: Common objects in context. In *Computer Vision—ECCV 2014: 13th European Conference, Zurich, Switzerland, September 6–12, 2014, Proceedings, Part V 13*, pages 740–755. Springer, 2014. 6
- [31] Shilong Liu, Zhaoyang Zeng, Tianhe Ren, Feng Li, Hao Zhang, Jie Yang, Qing Jiang, Chunyuan Li, Jianwei Yang, Hang Su, et al. Grounding dino: Marrying dino with grounded pre-training for open-set object detection. *arXiv preprint arXiv:2303.05499*, 2023. 6
- [32] Jian Ma, Junhao Liang, Chen Chen, and Haonan Lu. Subject-diffusion: Open domain personalized text-to-image generation without test-time fine-tuning. In *ACM SIGGRAPH 2024 Conference Papers*, pages 1–12, 2024. 2, 3
- [33] Alex Nichol, Prafulla Dhariwal, Aditya Ramesh, Pranav Shyam, Pamela Mishkin, Bob McGrew, Ilya Sutskever, and Mark Chen. Glide: Towards photorealistic image generation and editing with text-guided diffusion models. *arXiv preprint arXiv:2112.10741*, 2021. 2
- [34] Xichen Pan, Li Dong, Shaohan Huang, Zhiliang Peng, Wenhui Chen, and Furu Wei. Kosmos-g: Generating images in context with multimodal large language models. *arXiv preprint arXiv:2310.02992*, 2023. 3
- [35] Maitreya Patel, Sangmin Jung, Chitta Baral, and Yezhou Yang. λ -eclipse: Multi-concept personalized text-to-image diffusion models by leveraging clip latent space. *arXiv preprint arXiv:2402.05195*, 2024. 2, 3
- [36] Dustin Podell, Zion English, Kyle Lacey, Andreas Blattmann, Tim Dockhorn, Jonas Müller, Joe Penna, and Robin Rombach. Sdxl: Improving latent diffusion models for high-resolution image synthesis. *arXiv preprint arXiv:2307.01952*, 2023. 1, 2, 3, 6
- [37] Zeju Qiu, Weiyang Liu, Haiwen Feng, Yuxuan Xue, Yao Feng, Zhen Liu, Dan Zhang, Adrian Weller, and Bernhard Schölkopf. Controlling text-to-image diffusion by orthogonal finetuning. *Advances in Neural Information Processing Systems*, 36:79320–79362, 2023. 2
- [38] Alec Radford, Jong Wook Kim, Chris Hallacy, Aditya Ramesh, Gabriel Goh, Sandhini Agarwal, Girish Sastry, Amanda Aspell, Pamela Mishkin, Jack Clark, et al. Learning transferable visual models from natural language supervision. In *International conference on machine learning*, pages 8748–8763. PMLR, 2021. 2, 3, 6, 1
- [39] Aditya Ramesh, Prafulla Dhariwal, Alex Nichol, Casey Chu, and Mark Chen. Hierarchical text-conditional image generation with clip latents. *arXiv preprint arXiv:2204.06125*, 1 (2):3, 2022. 1, 2
- [40] Anton Razzhigaev, Arseniy Shakhmatov, Anastasia Maltseva, Vladimir Arkhipkin, Igor Pavlov, Ilya Ryabov, Angelina Kuts, Alexander Panchenko, Andrey Kuznetsov, and Denis Dimitrov. Kandinsky: an improved text-to-image synthesis with image prior and latent diffusion. *arXiv preprint arXiv:2310.03502*, 2023. 1
- [41] Scott Reed, Zeynep Akata, Xinchun Yan, Lajanugen Logeswaran, Bernt Schiele, and Honglak Lee. Generative adversarial text to image synthesis. In *International conference on machine learning*, pages 1060–1069. PMLR, 2016. 2
- [42] Jiawei Ren, Mengmeng Xu, Jui-Chieh Wu, Ziwei Liu, Tao Xiang, and Antoine Toisoul. Move anything with layered scene diffusion. In *Proceedings of the IEEE/CVF Conference on Computer Vision and Pattern Recognition*, pages 6380–6389, 2024. 2, 4
- [43] Robin Rombach, Andreas Blattmann, Dominik Lorenz, Patrick Esser, and Björn Ommer. High-resolution image synthesis with latent diffusion models. In *Proceedings of the IEEE/CVF conference on computer vision and pattern recognition*, pages 10684–10695, 2022. 1, 2, 3
- [44] Nataniel Ruiz, Yuanzhen Li, Varun Jampani, Yael Pritch, Michael Rubinstein, and Kfir Aberman. Dreambooth: Fine tuning text-to-image diffusion models for subject-driven generation. In *Proceedings of the IEEE/CVF conference on computer vision and pattern recognition*, pages 22500–22510, 2023. 2
- [45] Chitwan Saharia, William Chan, Saurabh Saxena, Lala Li, Jay Whang, Emily L Denton, Kamyar Ghasemipour, Raphael Gontijo Lopes, Burcu Karagol Ayan, Tim Salimans, et al. Photorealistic text-to-image diffusion models with deep language understanding. *Advances in neural information processing systems*, 35:36479–36494, 2022. 1, 2
- [46] Christoph Schuhmann, Romain Beaumont, Richard Vencu, Cade Gordon, Ross Wightman, Mehdi Cherti, Theo Coombes, Aarush Katta, Clayton Mullis, Mitchell Wortsman, et al. Laion-5b: An open large-scale dataset for training next generation image-text models. *Advances in Neural Information Processing Systems*, 35:25278–25294, 2022. 6
- [47] Takahiro Shirakawa and Seiichi Uchida. Noisecollage: A layout-aware text-to-image diffusion model based on noise cropping and merging. In *Proceedings of the IEEE/CVF Conference on Computer Vision and Pattern Recognition*, pages 8921–8930, 2024. 2, 4
- [48] Jiaming Song, Chenlin Meng, and Stefano Ermon. Denoising diffusion implicit models. *arXiv preprint arXiv:2010.02502*, 2020. 1, 2, 6
- [49] Yang Song, Jascha Sohl-Dickstein, Diederik P Kingma, Abhishek Kumar, Stefano Ermon, and Ben Poole. Score-based generative modeling through stochastic differential equations. *arXiv preprint arXiv:2011.13456*, 2020. 1, 2

- [50] Quan Sun, Yufeng Cui, Xiaosong Zhang, Fan Zhang, Qiyang Yu, Yueze Wang, Yongming Rao, Jingjing Liu, Tiejun Huang, and Xinlong Wang. Generative multimodal models are in-context learners. In *Proceedings of the IEEE/CVF Conference on Computer Vision and Pattern Recognition*, pages 14398–14409, 2024. 2, 3
- [51] Patrick von Platen, Suraj Patil, Anton Lozhkov, Pedro Cuenca, Nathan Lambert, Kashif Rasul, Mishig Davaadorj, Dhruv Nair, Sayak Paul, William Berman, Yiyi Xu, Steven Liu, and Thomas Wolf. Diffusers: State-of-the-art diffusion models. <https://github.com/huggingface/diffusers>, 2022. 1
- [52] Qixun Wang, Xu Bai, Haofan Wang, Zekui Qin, Anthony Chen, Huaxia Li, Xu Tang, and Yao Hu. Instantid: Zero-shot identity-preserving generation in seconds. *arXiv preprint arXiv:2401.07519*, 2024. 2, 3, 4, 1
- [53] Xudong Wang, Trevor Darrell, Sai Saketh Rambhatla, Rohit Girdhar, and Ishan Misra. Instancediffusion: Instance-level control for image generation. In *Proceedings of the IEEE/CVF Conference on Computer Vision and Pattern Recognition*, pages 6232–6242, 2024. 2, 3, 4, 7
- [54] X Wang, Siming Fu, Qihan Huang, Wangui He, and Hao Jiang. Ms-diffusion: Multi-subject zero-shot image personalization with layout guidance. *arXiv preprint arXiv:2406.07209*, 2024. 2, 3, 4, 5, 6, 7, 1
- [55] Yuxiang Wei, Yabo Zhang, Zhilong Ji, Jinfeng Bai, Lei Zhang, and Wangmeng Zuo. Elite: Encoding visual concepts into textual embeddings for customized text-to-image generation. In *Proceedings of the IEEE/CVF International Conference on Computer Vision*, pages 15943–15953, 2023. 2
- [56] Yinwei Wu, Xianpan Zhou, Bing Ma, Xuefeng Su, Kai Ma, and Xinchao Wang. Ifadapter: Instance feature control for grounded text-to-image generation. *arXiv preprint arXiv:2409.08240*, 2024. 2, 3, 4
- [57] Zhi-Fan Wu, Lianghua Huang, Wei Wang, Yanheng Wei, and Yu Liu. Multigen: Zero-shot image generation from multimodal prompts. In *European Conference on Computer Vision*, pages 297–313. Springer, 2024. 3
- [58] Jinheng Xie, Yuexiang Li, Yawen Huang, Haozhe Liu, Wentian Zhang, Yefeng Zheng, and Mike Zheng Shou. Boxdiff: Text-to-image synthesis with training-free box-constrained diffusion. In *Proceedings of the IEEE/CVF International Conference on Computer Vision*, pages 7452–7461, 2023. 2
- [59] Zhengyuan Yang, Jianfeng Wang, Zhe Gan, Linjie Li, Kevin Lin, Chenfei Wu, Nan Duan, Zicheng Liu, Ce Liu, Michael Zeng, et al. Reco: Region-controlled text-to-image generation. In *Proceedings of the IEEE/CVF Conference on Computer Vision and Pattern Recognition*, pages 14246–14255, 2023. 2
- [60] Hu Ye, Jun Zhang, Sibao Liu, Xiao Han, and Wei Yang. Ip-adapter: Text compatible image prompt adapter for text-to-image diffusion models. *arXiv preprint arXiv:2308.06721*, 2023. 2, 3, 4, 5, 1
- [61] Lvmin Zhang, Anyi Rao, and Maneesh Agrawala. Adding conditional control to text-to-image diffusion models. In *Proceedings of the IEEE/CVF International Conference on Computer Vision*, pages 3836–3847, 2023. 2
- [62] Youcai Zhang, Xinyu Huang, Jinyu Ma, Zhaoyang Li, Zhaochuan Luo, Yanchun Xie, Yuzhuo Qin, Tong Luo, Yaqian Li, Shilong Liu, et al. Recognize anything: A strong image tagging model. In *Proceedings of the IEEE/CVF Conference on Computer Vision and Pattern Recognition*, pages 1724–1732, 2024. 6
- [63] Yuxuan Zhang, Yiren Song, Jiaming Liu, Rui Wang, Jinpeng Yu, Hao Tang, Huaxia Li, Xu Tang, Yao Hu, Han Pan, et al. Ssr-encoder: Encoding selective subject representation for subject-driven generation. In *Proceedings of the IEEE/CVF Conference on Computer Vision and Pattern Recognition*, pages 8069–8078, 2024. 2, 3
- [64] Dewei Zhou, You Li, Fan Ma, Zongxin Yang, and Yi Yang. Migc++: Advanced multi-instance generation controller for image synthesis. *arXiv preprint arXiv:2407.02329*, 2024. 2, 5
- [65] Dewei Zhou, You Li, Fan Ma, Xiaoting Zhang, and Yi Yang. Migc: Multi-instance generation controller for text-to-image synthesis. In *Proceedings of the IEEE/CVF Conference on Computer Vision and Pattern Recognition*, pages 6818–6828, 2024. 2, 3, 4, 6, 7

MUSE: Multi-Subject Unified Synthesis via Explicit Layout Semantic Expansion

Supplementary Material

In this supplementary material, we provide more design details of our layout-controllable multi-subject synthesis (LMS) method MUSE, along with extensive experimental results. These include comparisons between our proposed MUSE and other LMS methods, evaluations of concatenated cross-attention (CCA) versus decoupled cross-attention (DCA), ablation studies on the progressive two-stage training strategy, and ablation experiments on the subject synthesis strength scale. Additionally, in the *MUSE_AttnProcessor.py* file, we provide the implementation of the final cross-attention operation that integrates both the CCA and DCA methods. This implementation is built using the diffusers [51] library.

A. More Details of Encoding Control Information

For the text for layout control and the images for subject synthesis, we use CLIP-ViT-L-14 and CLIP-ViT-G-14 [38] models for encoding, respectively.

For layout text features, we extract the class token from the CLIP model’s final output. For a class text like “dog”, the encoded feature has a size of [1,768]. Bounding box information is Fourier-encoded with a frequency of 16, producing a feature of size [1, 64]. These two features are concatenated along the feature dimension, resulting in a [1, 768+64] feature, which is further processed by an MLP to produce a fused grounding token of size [1,768]. The MLP consists of three linear layers with SiLU activation functions.

For image encoding, the straightforward approach is to use the same final class token output of CLIP encoding (size [1, 1280]) concatenated with bounding box features to create the grounding token. While sufficient for simple text class, this is inadequate for subject synthesis, as the class token lacks rich spatial information. Existing subject synthesis works like IP-Adapter [60], RealCustom [23], and InstantID [52] utilize shallower CLIP features, such as the last hidden states (size [256, 1664]), which offer ample spatial information. However, excessive spatial detail leads to redundancy in subject synthesis (e.g., copy-paste artifacts), especially since SDXL [36] itself uses only 77 tokens for text prompts control.

To address this, we adopt IP-Adapter-Plus’s approach: train 4 learnable tokens as queries, processed through four layers of perceiver attention, extracting compressed image features of size [4, 2048]. Directly concatenating bounding box information ([4, 2048+64]) into the tokens for MLP fusion degrades subject synthesis, as independently pro-

cessed tokens may produce inconsistent results due to neural network black-box behavior. Instead, we independently encode the Fourier-transformed bounding box information into [1, 2048] through an MLP, and add this layout encoding to each image token, achieving coherent grounding tokens. Mapping the dimension of the image grounding token to 2048 is intended to initialize the mapping layer parameters in DCA using those from the pretrained model, thereby reducing the training difficulty of the model.

B. More Details of Experimental Setup

Since the data samples used in both training and testing contain multiple subjects, we set the number of subjects per sample to 10. For samples with more than 10 subjects, we select the 10 largest bounding box areas. For samples with fewer than 10 subjects, we use padding by introducing trainable empty tokens to maintain 10 subjects. These include text, image, and coordinate features. During training, we randomly drop captions for images and conditions (e.g., subject texts, images and bounding boxes) for MUSE with a 0.1 probability to enhance robustness.

Regarding the loss function, we maintain consistency with the original pre-trained model. The diffusion network is trained to accurately predict added noise under additional multiple control conditions.

For each test experiment, we use five random seeds and report the average results.

C. More Qualitative Experiment Results

Fig. 8 provides more qualitative comparisons of our method against other LMS approaches, including GLIGEN [29] and MS-Diffusion [54], on the MS-Bench-Random dataset. Our approach consistently demonstrates superior performance in both layout control and multi-subject synthesis.

D. More Ablation experiments on Training Strategies

Fig. 9 presents qualitative results on the MS-Bench-Random dataset, comparing our progressive two-stage LMS framework with models trained using the full-DCA method and single-stage training combining CCA and DCA method. Our proposed framework achieves both accurate layout control and effective subject synthesis. The results confirm that our proposed progressive framework is more suitable for LMS tasks.

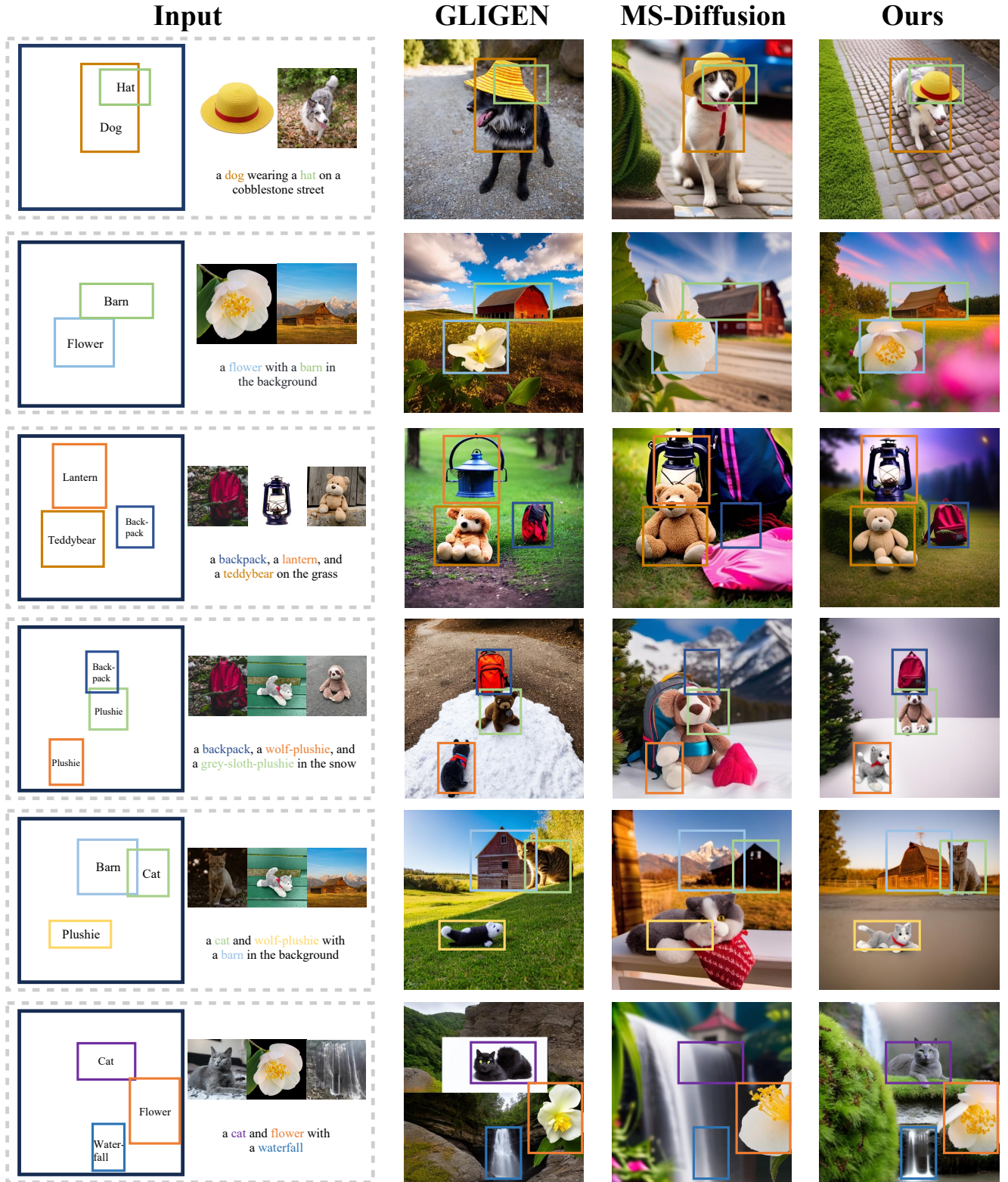


Figure 8. Qualitative experiments on MS-Bench-Random. Our method demonstrates strong LMS performance across various conditions, showing good practical applicability in real-world.

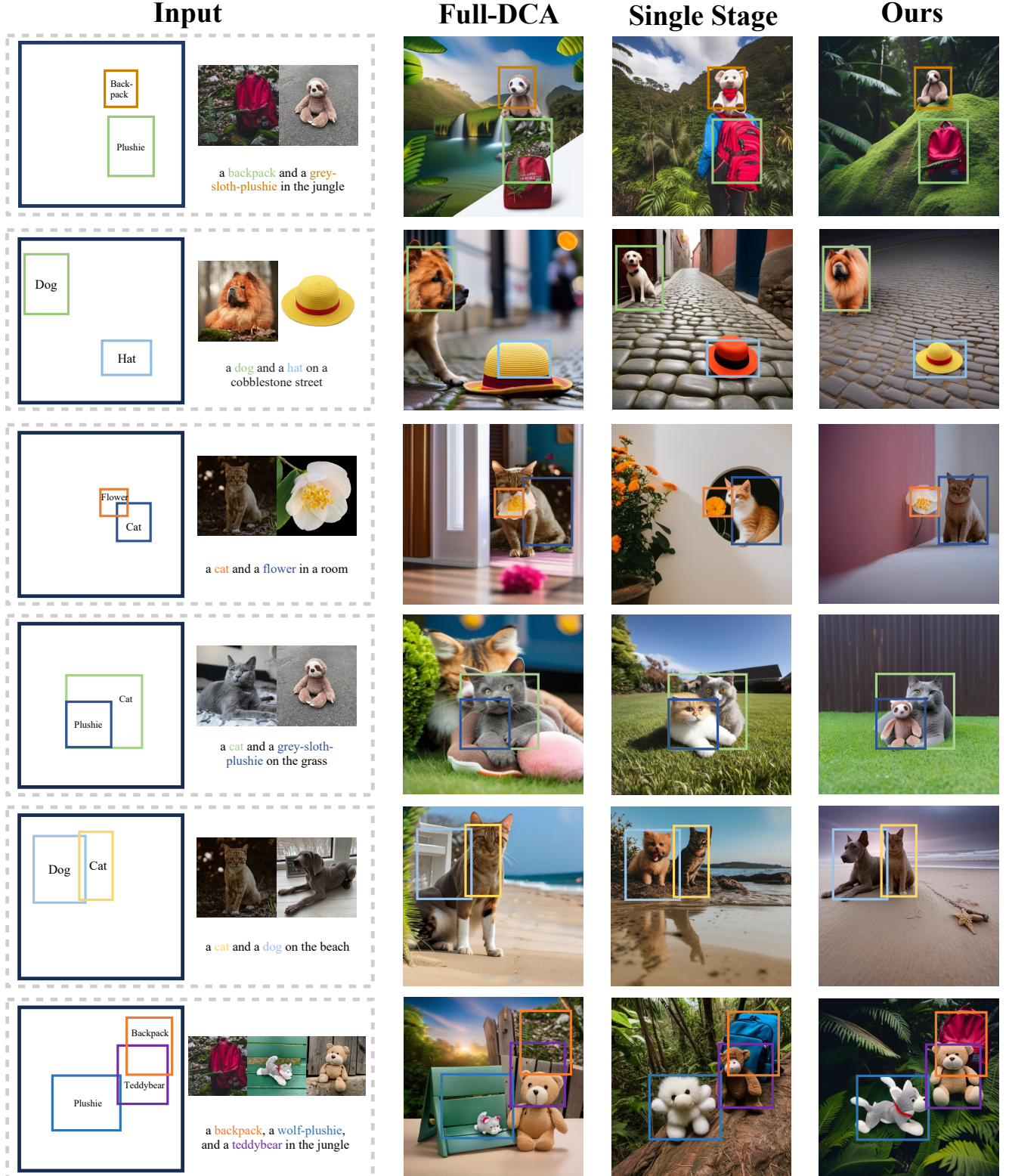


Figure 9. Ablation study on training strategies conducted on MS-Bench-Random. It shows that using both CCA and DCA methods along with our proposed progressive two-stage training strategy significantly improves performance on the LMS task.

Scale	MS-Bench				MS-Bench-Random			
	CLIP-T	CLIP-I-I	SR-0.6	SR-0.65	CLIP-T	CLIP-I-I	SR-0.6	SR-0.65
0.6	0.328	0.811	0.878	0.790	0.327	0.769	0.871	0.712
0.8	0.323	0.827	0.890	0.819	0.321	0.779	0.894	0.755
1.0	0.313	0.832	0.889	0.822	0.310	0.782	0.897	0.763

Table 5. Ablation experiments on the subject synthesis strength scale. The evaluated metrics include CLIP-T, CLIP-I-local (abbreviated as CLIP-I-I), and LMS Success Rate (SR), determined using CLIP-I-local score thresholds of 0.6 and 0.65, referred to as SR-0.6 and SR-0.65, respectively.

E. Ablation experiments on Subject synthesis Strength Scale

We conducted ablation experiments on the subject synthesis strength scale λ . While the default scale is set to 0.8, we provide results for $\lambda = 0.6$ and $\lambda = 1.0$ on the MS-Bench-Random dataset. Quantitative comparisons are shown in Tab. 5.

The results indicate that high subject synthesis strength scale can weaken text-following ability, while low strength scale reduces subject synthesis quality. A balanced value achieves optimal performance.